EXPERIMENTAL NEUROLOGY **146,** 212–229 (1997)
ARTICLE NO. EN976522

3-Nitropropionic Acid Neurotoxicity: Visualization by Silver Staining and Implications for Use as an Animal Model of Huntington's Disease

Paul J. Miller[1] and Laszlo Zaborszky[2]

Center for Molecular and Behavioral Neuroscience, Rutgers, The State University of New Jersey, Newark, New Jersey 07102

The neuronal damage produced by the mitochondrial toxin 3-nitropropionic acid (3NPA) has been suggested to replicate much of the neuropathology seen in Huntington's disease (HD) and therefore might be used in an animal model. We investigated the susceptibility to this toxin of different neuronal populations in addition to the commonly studied caudate putamen by injecting 3NPA into seven different brain regions as well as systemically. After different survival times, rats were intracardially perfused, brain sections were processed with the Gallyas silver technique, and impregnated neurons were mapped with a computerized microscope. Intracerebral administration of 3NPA resulted in a lesion, the center of which was devoid of tissue while the area was surrounded by a halo of Golgi-like impregnated neurons. In addition to local damage, rats receiving microinjections into the frontal cortex, caudate putamen, basal forebrain, and amygdala displayed argyrophilic neurons in the thalamus corresponding to the topography of thalamofugal neurons projecting to the individual injection sites. On the other hand, negligible secondary damage was seen after injections into the internal capsule, thalamus, or substantia nigra, implicating that thalamofugal axons are especially vulnerable to the local effect of this toxin. Two and a half days after systemic administration of 3NPA, a diffuse argyrophilic neuronal reaction was seen in the dorsolateral part of the caudate putamen, together with a more regionally selective staining of neurons in different cortical areas and the hippocampus. These morphopathological changes were also accompanied by motor deficits. The affected neurons in the cortical regions were primarily in those layers (V and VI) and areas (medial prefrontal, caudal insular/perirhinal, and ventral temporal) that do not project toward the lesioned striatal area; therefore, the cortical pathology may represent another primary site of action of the toxin. Among the affected neurons in the hippocampal complex were pyramidal neurons in the CA1 region as well as various neurons in the CA3 region and dentate hilar area. These studies suggest that a combination of 3NPA administration and a sensitive silver-impregnation method may unravel the potential site of primary neuronal damage in this animal model. Furthermore, these findings may contribute to the understanding of how the disease progresses in HD from the originally affected neuronal population(s) by the recruitment of closely related systems and pathways.

INTRODUCTION

Huntington's disease (HD),[3] an autosomal dominant disorder showing complete penetrance, results from a trinucleotide expansion on chromosome 4 (44). The common chorea seen in patients may result from the loss of enkephalin- and substance P-containing, medium-sized spiny striatal projection neurons that send efferents to the globus pallidus and substantia nigra pars reticulata (19, 32, 71). In contrast, medium-sized

[1] Present address: Amgen, Inc., Department of Neuroscience, 1840 DeHavilland Drive, Thousand Oaks, CA 91320.

[2] To whom correspondence should be addressed at the Center for Molecular & Behavioral Neuroscience, Rutgers University, 197 University Avenue, Newark, NJ 07102. Fax: (201) 648-1272.

[3] Abbreviations used: 3NPA, 3-nitropropionic acid; 3V, third ventricle; ac, anterior commisure; Acb, accumbens nucleus; Ai, agranular insular cortex; AD, anterodorsal thalamic nucleus; AH, anterior hypothalamic area; AM, anteromedial thalamic nucleus; AV, anteroventral thalamic nucleus; BF, basal forebrain; BL, basolateral amygdaloid nucleus; Bst, bed nucleus stria terminalis; CA3, field CA3 of Ammon's horn; Ce, central amygdaloid nucleus; CL, centrolateral thalamic nucleus; CM, centromedial thalamic nucleus; CP, caudate putamen; ec, external capsule; GP, globus pallidus; Gu, gustatory cortex; FC, frontal cortex; HD, Huntington's disease; HDB, horizontal limb diagonal band; ic, internal capsule; lo, lateral olfactory tract; LD, laterodorsal thalamic nucleus; LHb, lateral habenular nucleus; LV, lateral ventricle; opt, optic tract; ox, optic chiasm; MD, mediodorsal thalamic nucleus; MG, medial geniculate nucleus; MHb, medial habenular nucleus; M1, primary motor cortex; M2, supplemental motor cortex; NADH; nicotinamide adenine dinucleotide phosphate, reduced; NMDA, *N*-methyl-D-aspartate; NOS, nitric oxide synthase; Pir, piriform cortex; PT, parataenial thalamic nucleus; Re, reuniens thalamic nucleus; Rh, rhomboid thalamic nucleus; rf, rhinal fissure; Rt, reticular thalamic nucleus; SC, superior colliculus; SI, substantia innominata; sm, stria medullaris thalami; SNc, substantia nigra pars compacta; S1, primary somatosensory cortex; S2, supplemental somatosensory cortex; VAL, ventral anterior–lateral thalamic complex; VL, ventrolateral thalamic nucleus; VM, ventromedial thalamic nucleus; VP, ventral pallidum; VPM, ventral posteromedial thalamic nucleus; VPL, ventral posterolateral thalamic nucleus; ZI, zona incerta.

0014-4886/97 $25.00

aspiny interneurons containing nicotinamide adenine dinucleotide phosphate (NADPH) diaphorase, neuropeptide Y, and somatostatin and large aspiny cholinergic neurons are relatively spared (13, 19, 25, 47, 64). Furthermore, there is some evidence for damage to other brain areas, including the cortex and thalamus (20, 33, 40, 49, 53, 76).

Intrastriatal or systemic administration of axon-sparing excitotoxins including kainic acid, quinolinic acid, and ibotenic acid in rodents and primates has been shown to destroy spiny striatal projection neurons and result in similar hyperkinetic movements as seen in HD (8, 17, 25, 37, 54, 74). Recently, 3-nitropropionic acid (3NPA), a plant fungal toxin which inactivates mitochondrial succinate dehydrogenase (14), has been used for studying the HD pathology. Ingestion of this toxin by eating contaminated sugar cane results in basal ganglia lesions and a marked dystonia in children (52). Similar behavioral and neuropathological changes were found in rats and mice after intrastriatal and systemic administration (7, 11, 31).

Although the striatal damage produced by 3NPA in rats has been previously described (7, 12, 36, 86), the mechanism of action of this toxin is still unclear. Furthermore, whether other neuronal populations in addition to striatal neurons can be affected by 3NPA has not been examined. Therefore we injected 3NPA into areas related to basal ganglia circuits, including the frontal cortex (FC), substantia nigra, thalamus, and amygdala. We also investigated whether 3NPA could affect neurons through uptake into fibers of passage. Finally, we examined for neuronal vulnerability throughout the forebrain following systemic 3NPA administration.

The silver impregnation technique developed by Gallyas *et al.* (28) has been shown to produce a Golgi-like staining of neurons ("argyrophilic" or "dark" neurons) affected by various types of neuronal insult. These include ischemia, traumatic brain injury, and neurotoxin-induced damage (28, 29, 38), disease states which have been linked to both necrotic and apoptotic cell death (5, 24, 45, 68). This sensitive silver method was employed to detect the neuronal populations compromised by 3NPA administration as well as to follow the time course of 3NPA-induced morphopathological changes.

MATERIALS AND METHODS

Animals

Fifty adult male Sprague–Dawley rats (Zivic–Miller, Pittsburgh, PA) weighing 275–325 g were used in this study. Animals were housed on a 12/12 light/dark cycle in a temperature- and humidity-controlled room. Food and water were available *ad libitum*. All animal procedures were conducted in accordance with the *NIH Guide for the Care and Use of Laboratory Animals.*

Drug Administration

For microinjection, 3NPA (Sigma Chemical Co.) was dissolved in 0.1 *M* phosphate buffer. A 27-gauge needle connected via PE-20 tubing (Clay Adams) to a 5-µl Hamilton syringe was used to deliver 3NPA (500 nmol). Rats were anesthetized with sodium pentobarbital (50 mg/kg, ip) and stereotaxic (David Kopf Instruments) microinjections were aimed at the following coordinates: caudate putamen (AP +0.5, LM −2.0, DV −5.0), basal forebrain (AP −0.8, LM −2.5, DV −7.6, ipsilateral injection; or AP −0.8, LM +3.6, DV −9.7, angle = 38.5°, contralateral injection), internal capsule (AP −1.6, LM +3.0, DV −8.9, angle = 42.0°, contralateral injection), thalamus (AP −2.12, LM +3.6, DV −7.7), frontal cortex (AP +3.2, LM −0.6, DV −2.8 and AP +3.2, LM −3.8, DV −2.3), amygdala (AP −3.3, LM −4.8, DV −7.0), and substantia nigra (AP −5.3, LM −2.0, DV −7.8) according to Paxinos and Watson (65). Between four and six animals were used for each microinjection lesion group.

Injection rate was controlled by a computerized pump (Harvard Apparatus). Frontal cortex received two injections of 0.5 µl each at a rate of 0.1 µl/min and amygdala and substantia nigra received 0.4 µl at a rate of 0.1 µl/min. All other brain areas received a volume of 0.1 µl at a rate of 0.02 µl/min. Following 3NPA injections, the needle was left in place an additional 2 min before slow withdrawal from the brain. The same volume of the vehicle (0.1 M phosphate buffer) was injected into the contralateral hemisphere as controls. All rats were perfused 5 or 15 days following surgery.

For systemic injections, 3NPA injections were given at a dose of 10 mg/kg, twice daily at 12-h intervals (a total of five injections). Since many animals became severely sick or died during this treatment, the remaining animals were perfused approximately 60 h after the first injection.

To increase chances of survival and examine potential long-term effects, several animals were given a reduced dose of 3NPA ip (rather than a total of 20 mg/kg daily, only 15 mg/kg once daily was given) over a period of 3 days and were perfused 2 weeks following the end of the 3NPA treatment. Half of the animals died within the first week; the remaining animals were perfused at the end of the second week.

Perfusion and Tissue Processing

Rats were deeply anesthetized with pentobarbital and intracardially perfused with a buffered paraformaldehyde/glutaraldehyde solution (28). Brains were removed from the skull 16–24 h later, placed in the same fixative for 3 days, and then transferred to a 30% sucrose/fixative solution for an additional 3 days. Tissue sections were cut at 60 µm on a freezing microtome and were processed according to a previously described

silver technique (28). Briefly, sections were dehydrated in a graded 1-propanol series and incubated in an esterifying solution for 16 h at 56°C. Thereafter, sections were rehydrated, treated in 8% acetic acid for 10 min, and placed into a silicotungstate developer. The reaction was terminated by placing the sections in 1% acetic acid for 30 min. Adjacent sections were stained for Nissl to aid in delineating brain structures and to examine potential cell loss.

Silver-impregnated neurons were mapped using a computerized microscope and the Neurolucida software (MicroBrightField, Inc.). These Neurolucida images were then carefully aligned and overlaid on the corresponding brain maps from the Swanson atlas (79).

RESULTS

Effect of Intracerebral Microinjection of 3NPA

The locations of 3NPA microinjection sites are summarized in Fig. 1. All lesions consisted of a center of complete cell loss usually surrounded by several silver-impregnated ("dark") neurons. In several instances we observed dark neurons outside of the vicinity of the injection, demonstrating an additional, secondary neuronal insult. Table 1 summarizes the various injection paradigms and locations of silver-impregnated neurons.

3NPA lesions in the frontal cortex (FC; Fig. 1a), caudate putamen (CP) (Fig. 1b), basal forebrain ("ipsilateral" BF lesion, Fig. 1c; "contralateral" BF injection, Fig. 1d), and amygdaloid body (Fig. 1g) resulted in secondary argyrophilic neuronal reaction in thalamic nuclei. On the other hand, injections into the internal capsule (Fig. 1e), thalamus (Fig. 1f), or substantia nigra (Fig. 1h) did not cause dark neuronal staining in areas outside the immediate vicinity of the lesion site.

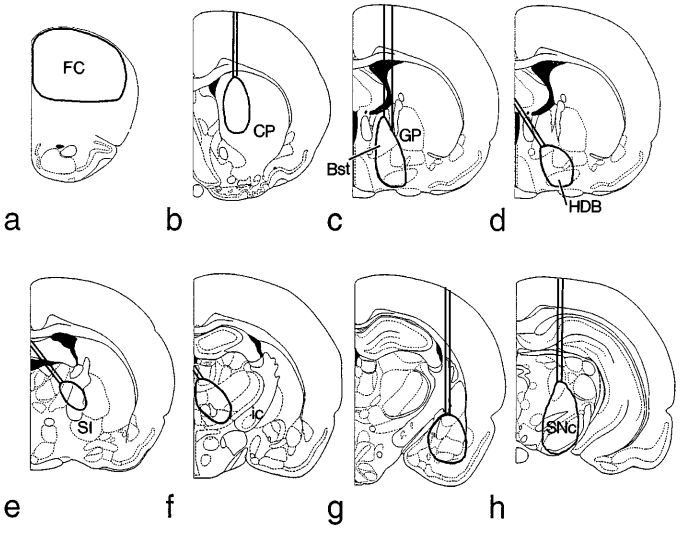

FIG. 1. Schematic figures adapted from Paxinos and Watson (65) illustrating lesions following intracerebral injections of 3NPA. The thick black line in each representative case encompasses the area of immediate neuronal damage; the double lines represent the shaft of the microinjection needle. (a) Frontal cortex lesion. (b) Caudate putamen lesion. (c) Basal forebrain lesion, needle entering from the ipsilateral side. (d) Basal forebrain lesion, needle entering from the contralateral side. (e) Internal capsule lesion. (f) Thalamus lesion. (g) Amygdala lesion. (h) Substantia nigra lesion.

The 3NPA injection into CP (Fig. 1b) was located in its medial one-third, and the microinjection needle caused minimal damage to the overlying cortex (few, if any, dark cells were observed around the needle track) and the cingulate bundle. Animals receiving striatal 3NPA microinjections displayed silver-impregnated neurons in several thalamic nuclei, including the anteroventral, mediodorsal, laterodorsal, and intralaminar nuclei (Fig. 2).

In the ipsilateral BF cases (Fig. 1c), the injections were centered in an area encompassing the horizontal limb of the diagonal band, substantia innominata, lateral part of the bed nucleus of the stria terminalis, and lateral hypothalamic area. The shaft of the microinjection needle penetrated the medial part of the CP, resulting in a "spillover" of the toxin and the presence of several dark neurons in this area. Affected neurons could be seen in the same thalamic nuclei as was found in striatal (CP) cases; in addition, an argyrophilic reaction was seen in the ventromedial and paraventricular thalamic nuclei. Figure 3 illustrates the distribution and characteristics of argyrophilic neurons in the thalamus in a coronal section following ipsilateral 3NPA injection into the BF. In the cases where 3NPA was injected from the contralateral hemisphere, impregnated neurons were observed in the same thalamic nuclei as after ipsilateral approach, except in the anterodorsal and ventromedial nuclei that did not contain any impregnated neurons. Also, the number of affected neurons was less after contralateral injections.

Two large 3NPA injections were directed at the same anterior–posterior level in the frontal cortex, encompassing from medial to lateral the anterior cingulate cortex, the supplemental motor area (M2), the rostral and deep parts of the lateral frontal cortex (primary motor area, M1), with a slight involvement of the prelimbic (medial prefrontal) and the dorsal agranular insular (lateral prefrontal) cortices (Fig. 1a). In addition, superficial fibers of the forceps minor (corpus callosum) and the dorsalmost part of the CP were also damaged. In these cases, silver-impregnated neurons and cellular debris were particularly noticeable in the mediodorsal, ventrolateral, and ventromedial thalamic nuclei. Additional areas containing affected cells included medial CP and globus pallidus. Figure 4 shows the distribution of dark neurons at two levels of the thalamus.

The amygdaloid injection was centered in the lateral and basolateral amygdaloid nuclei (Fig. 1g). The lesion also included the dorsal portion of the central nucleus and the caudoventral part of the putamen. Dark neu-

TABLE 1

Distribution of Silver-Impregnated Neurons Following Intracerebral and Systemic Injections of 3NPA

	Site of injection and survival time									
	Frontal CTX		Striatum		BFi	BFc	Amygdala		Systemic (ip)	
Location of "dark" cells	5 days	15 days	5 days	15 days	5 days	15 days	5 days	15 days	2.5 days	15 days
Thalamus										
Anterodorsal	−	−	+−	+−, *	++	−	−	−	−	−
Anteromedial	−	−	++	+−, *	+++	+−	−	−	−	−
Anteroventral	−	−	+	+, *	+++	+−	−	−	−	−
Laterodorsal	−	−	+	+−, *	+	+−	−	−	−	−
Ventromedial	−	+, *	−	−	+−	−	−	−	−	−
Ventrolateral	−	+, *	+−	−	−	−	−	−	−	−
Ventrobasal	−	−, *	−	−	−	−	+−	−		
Mediodorsal	−	+, *	++	+, *	++	+	−	−	−	−
Intralaminar	−	−	++	+, *	++	++	−	−	−	−
Paraventricular	−	−	−	−	++	+	−	−	−	−
Rheuniens	−	−	+	+−, *	+++	+−	−	−	−	−
Rhomboid	−	−	−	−	+	−	−	−	−	−
Medial geniculate	−	−	−	−	−	−	++	+−, *	−	−
Cortex										
Frontal/motor	i.s.	i.s.	−	−	−	−	−	−	+	−
Parietal/sensory (r)	−	−	−	−	−	−	−	−	+	−
Parietal/sensory (c)	−	−	−	−	−	−	−	−	++++	−
Temporal/auditory	−	−	−	−	−	−	−	−	+++	−
Occipital/visual	−	−	−	−	−	−	−	−	+++	−
Prefrontal	i.s.	i.s.	−	−	−	−	−	−	+++	−
Cingulate	i.s. (r)	i.s. (r)	−	−	−	−	−	−	++	−
Piriform	−	−	−	−	−	−	−	−	+−	−
Entorhinal	−	−	−	−	−	−	−	−	++	−
Insular (r)	−	−	−	−	−	−	−	−	++	−
Insular (c)	−	−	−	−	−	−	−	−	++++	−
Claustrum	−	−	−	−	−	−	−	−	+	−
Striatum	+−	+−	i.s.	i.s.	−	−	−	−	++++	+−
Hippocampus	−	−	−	−	−	−	−	−	+	+−
Amygdala	−	−	−	−	−	−	i.s.	i.s.	+−	−

Note. Abbreviations: *, neuronal debris; i.s., 3NPA injection site; c, caudal; r, rostral; CTX, cortex; BFi, basal forebrain ipsilateral; BFc, basal forebrain contralateral. Rating scale: mean/unilateral structure/per section: −, no cells; +−, occasional/1 cell; +, 2–5 cells; ++, 6–10 cells; +++, 11–20 cells; ++++, above 20 cells.

rons were seen in several thalamic nuclei, including the medial part of the medial geniculate body, the suprageniculate nucleus, and the ventrobasal complex.

Many impregnated neurons showed a full Golgi-like staining of the perikaryon and dendritic processes after a short survival time (5 days); however, the presence of an uneven staining of the perikaryon (arrowhead in Fig. 3e) and corkscrew-like dendrites (asterisk in Fig. 3d) indicated an early pathological change. After a longer survival time (15 days), many neurons were in an advanced stage of degeneration, and there was neuronal debris present, characterized by shrunken and/or disintegrated cell bodies and dendrites. In other words, there were fewer fully stained neurons and more debris 15 days following CP and amygdala 3NPA injection, while in cases with FC lesions, silver-impregnated neurons and debris were observed only following this longer survival time and no staining was observed at the 5-day time point.

Since neurons or fibers passing through the injection area are also compromised resulting in anterograde degeneration of their preterminal and terminal portions, in fortuitous cases, the input to the area containing the affected neurons can also be demonstrated by applying this silver method (Fig. 5).

Animals receiving vehicle injections occasionally had only one or two dark neurons in the thalamus. There were no readily apparent motor changes observed in any of the rats receiving intracerebral injections of 3NPA and all animals survived the appropriate planned survival times.

Effect of Systemic Injection of 3NPA

Following two ip injections of 3NPA, rats displayed a marked dystonia and rigidity. Five systemic injections of 3NPA resulted in immobility accompanied by widespread bilateral dark neuronal staining. The most

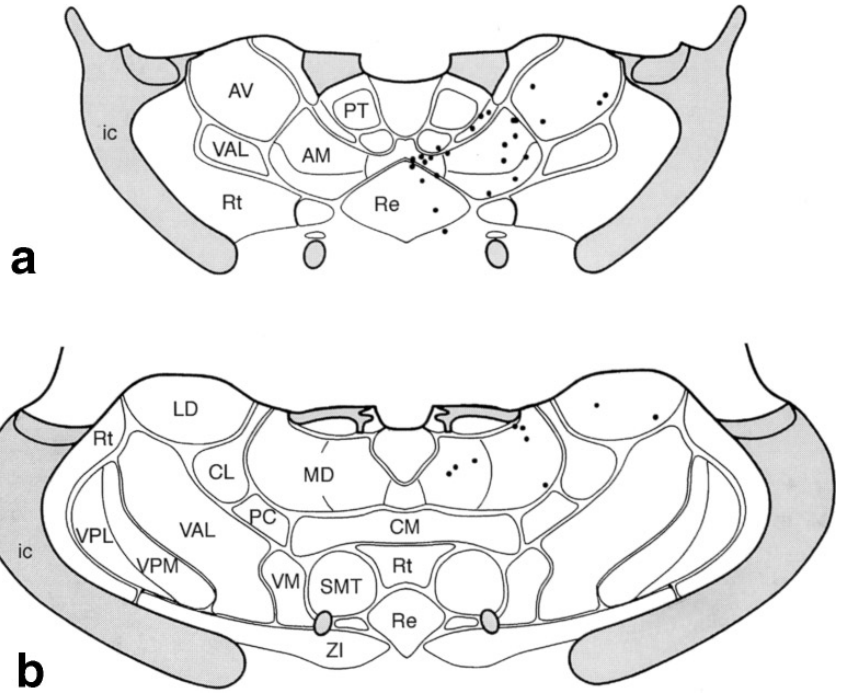

FIG. 2. Schematic figures adapted from Swanson (79) illustrating the distribution of dark neurons in the thalamus following intracerebral injection of 3NPA into the caudate putamen. Dots represent individual silver-impregnated cells. (a) Rostral section, approximately 1.5 mm behind bregma. (b) Caudal section, approximately 2.5 mm behind bregma.

heavily affected area was the CP, although the size of the damage was variable in each animal. Within the CP there was a spherical area occupying about two-thirds to three-fourths of the lateromedial CP and containing stained neurons, axons, and dendrites in its dense peripheral shell which was about 200 μm thick (Fig. 6a). Inside this shell only few neurons were impregnated, usually showing advanced degeneration; in addition many impregnated axons were seen especially in the bundles of the internal capsule. Nissl staining on adjacent sections revealed a reduction in cell density inside this shell of dark neurons (Fig. 6b). Parts of the lateral striatal artery inside or outside of the demarcated zone were often occluded. Although the size of this striatal injury showed some variation, the medial part of the CP and the shell of the nucleus accumbens were always free of argyrophilic neurons.

The distribution of silver-impregnated neurons following systemic 3NPA injections is shown in the series of coronal sections of Fig. 7. Particularly heavy neuronal staining can be seen in the deep layers (laminae V and VI) of the medial prefrontal cortex, the insular cortex including the claustrum, perirhinal, auditory, and ventral temporal areas. A few impregnated neurons were seen in the M1/S1 border. More caudally, particularly heavy labeling was observed in layers V and VI of all neocortical regions and the lateral entorhinal cortex. Occasionally, a few impregnated pyramidal neurons were also found in layer III (Fig. 7). Figure 8a shows the distribution of dark neurons in the parietal and temporal cortices. As can be seen, these silver-impregnated pyramidal neurons possess an abundance of spines (as shown by arrows in the figures), although the corkscrew-like dendrites suggest they are in an early phase of degeneration. Figure 9 shows further examples of silver-impregnated neurons from the temporal cortex from the same animal. Compared to neurons shown in Fig. 8, these dark neurons demonstrate a more advanced stage of degeneration, such as partial impregnation of the perikaryon (Fig. 9c) and beaded, disintegrating dendrites, and spines were no longer visible (Fig. 9e).

In cases where the dense striatal halo penetrated through the corpus callosum and insular cortex and most of the CP was involved except its most medial and caudal portions, a few impregnated neurons were also seen in the ventral part of the globus pallidus and many pyramidal neurons in layer III of the neocortical areas showed argyrophilia.

The hippocampal CA1 and CA3 fields and dentate gyrus also contained affected neurons (Fig. 10). The subiculum often contained an occluded capillary surrounded by impregnated pyramidal cell bodies. The stratum lacunosum moleculare was often densely packed with stained apical dendrites of pyramidal neurons. A few CA3c pyramidal neurons and dentate granule cells were also impregnated together with the characteristic staining of mossy fibers. Within the

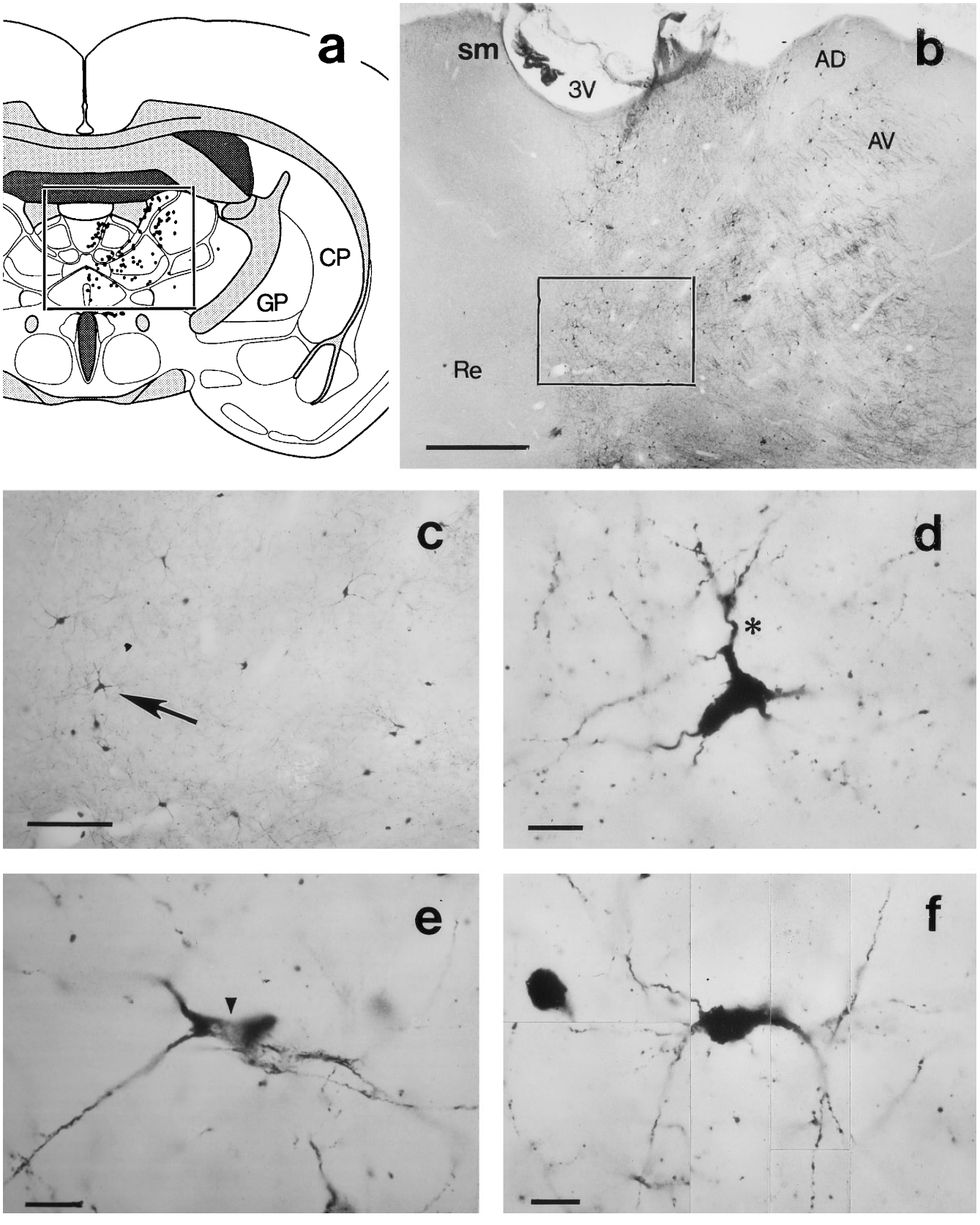

FIG. 3. Distribution of affected neurons in the thalamus following injection of 3NPA into the basal forebrain from the ipsilateral side. (a) Schematic showing location of dark neurons in the thalamus. Dots represent individual silver-impregnated cells. (b) Widespread distribution of silver-impregnated cells, boxed area from (a). (c) Arrow points to a dark neuron from the boxed area in (b). (d) Dark neuron taken from (c) (arrow) under higher magnification. (e and f) Representative dark thalamic neurons. Arrowhead, uneven staining of perikaryon. Asterisk, corkscrew-like dendrite. Scale bar: b, 500 μm; c, 100 μm; d–f, 10 μm.

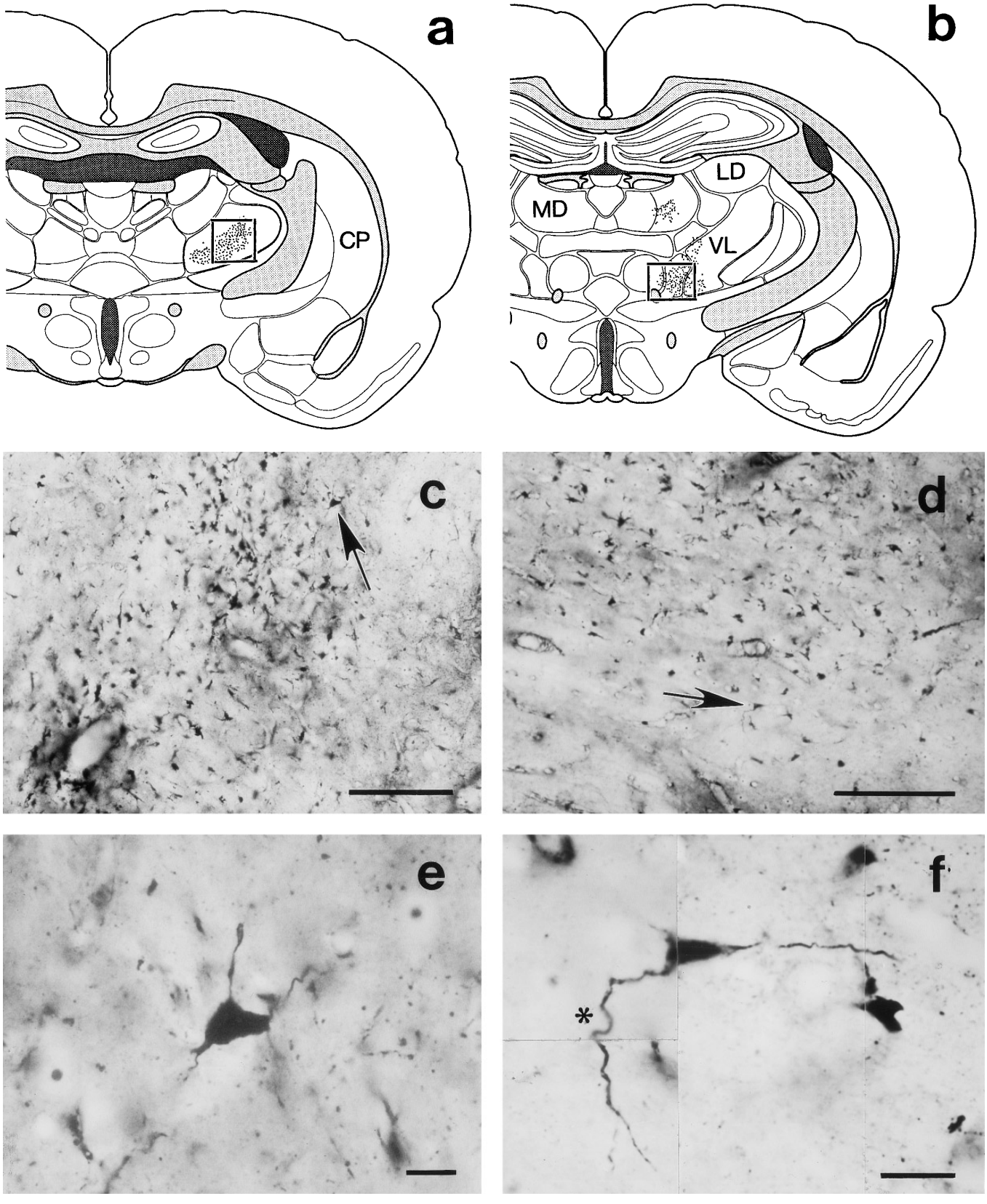

FIG. 4. 3NPA-induced neuronal damage in the thalamus following frontal cortex microinjection. (a and b) Diagrams of dark cells in the thalamus, plotted from corresponding coronal sections using the Neurolucida system and the Swanson atlas (79). Dots represent silver-impregnated neurons or cellular debris. (c and d) Low-magnification photographs of boxed areas in (a) and (b). (e and f) High-magnification photographs of dark cells, taken from above (c, arrow) and below (d, arrow), respectively. Asterisk, corkscrew-like dendrite. Scale bar: c and d, 100 μm; e and f, 10 μm.

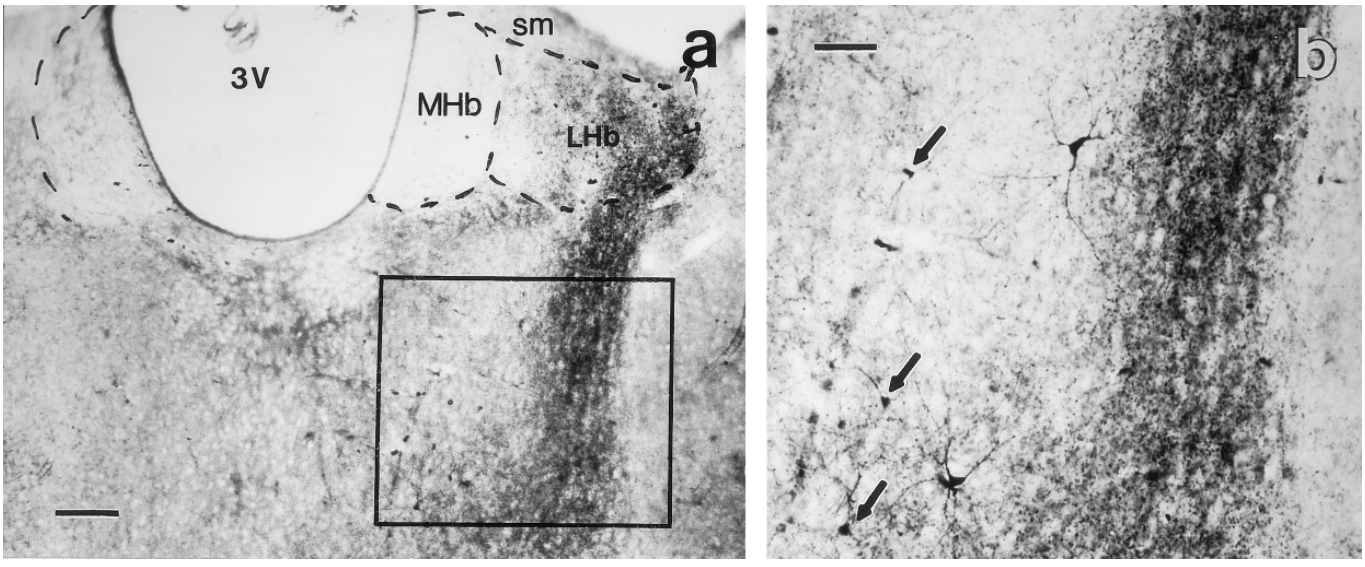

FIG. 5. Degenerating cell bodies and affected fibers in the dorsomedial thalamic nucles following 3NPA injection into basal forebrain from the contralateral side. (a) Low-magnification photomicrograph illustrating the mediodorsal thalamic nucleus. (b) High-magnification image of boxed area from (a) showing dark neurons and degenerating fibers/terminals. Several dark neurons are visible, some labeled with arrows. Note the well-defined pattern of dense terminal degeneration in the central part of this nucleus. Scale bar: a, 50 µm; b, 100 µm.

patchy regions, a few inhibitory interneurons were also impregnated. Although the thalamus often contained thrombotic vessels, only a few animals showed diffuse argyrophilic reaction in the posterior portion of the laterodorsal nucleus and adjoining posterior nuclei. This damage was similar to the dense striatal spherical staining of cells and dendrites and axons within the halo.

To examine the long-term effects of systemic 3NPA administration, several animals were given the reduced dosage of 3NPA ip (to increase chances of survival) over a period of 3 days and were perfused 2 weeks following the end of the 3NPA treatment. On Day 4, all animals showed visible motor deficits and were given sc glucose injections to improve chances of survival. Half of the animals died within the first week, but by the end of the second week, the remaining half appeared to possess normal motor abilities. Following perfusion and dark neuronal staining, there were only a few cells in the CP, cortex, and hippocampus, a drastic reduction in staining seen compared with the animals receiving the higher dose of 3NPA.

DISCUSSION

We have examined the neurotoxic damage induced by intracerebral and intraperitoneal delivery of 3NPA in rats, screening for neuronal populations that are vulnerable to this toxin. Our studies provide evidence that (1) following intracerebral administration of 3NPA, thalamofugal neurons are especially sensitive to this toxin when delivered into their potential target areas; (2) following systemic administration of 3NPA, in addition to the known striatal damage, a substantial number of cortical and hippocampal neurons are also compromised; and (3) the Gallyas silver-impregnation technique proved to be a sensitive method for defining the precise location and the time course of morphopathological changes of affected neurons.

Neurotoxic Risk Assessment

Different animal models of HD are useful for revealing the potential primary site of neuronal damage as well as for understanding the disease progression. The superior sensitivity of silver techniques to detect morphopathological changes in the brain compared to traditional Nissl staining has been known for decades (9). An example of the dramatic difference between 3NPA-induced striatal cell damage as revealed by the Gallyas silver method and Nissl staining can be observed by comparing Fig. 6a with Fig. 6b. Furthermore, smaller differences are still readily apparent after silver staining, such as with the silver-impregnated cortical neurons affected by 3NPA (Figs. 7–9); these impaired neurons in a similar experimental paradigm using Nissl staining could not be demonstrated (7). Although silver staining was recently used in combination with 3NPA administration (4), due to the fact that the particular silver technique was developed primarily for detecting degeneration of axon terminals (27), the consequent lack of staining of the somatodendritic domain prevented firm conclusions to be drawn as to identity of neuronal populations affected by 3NPA.

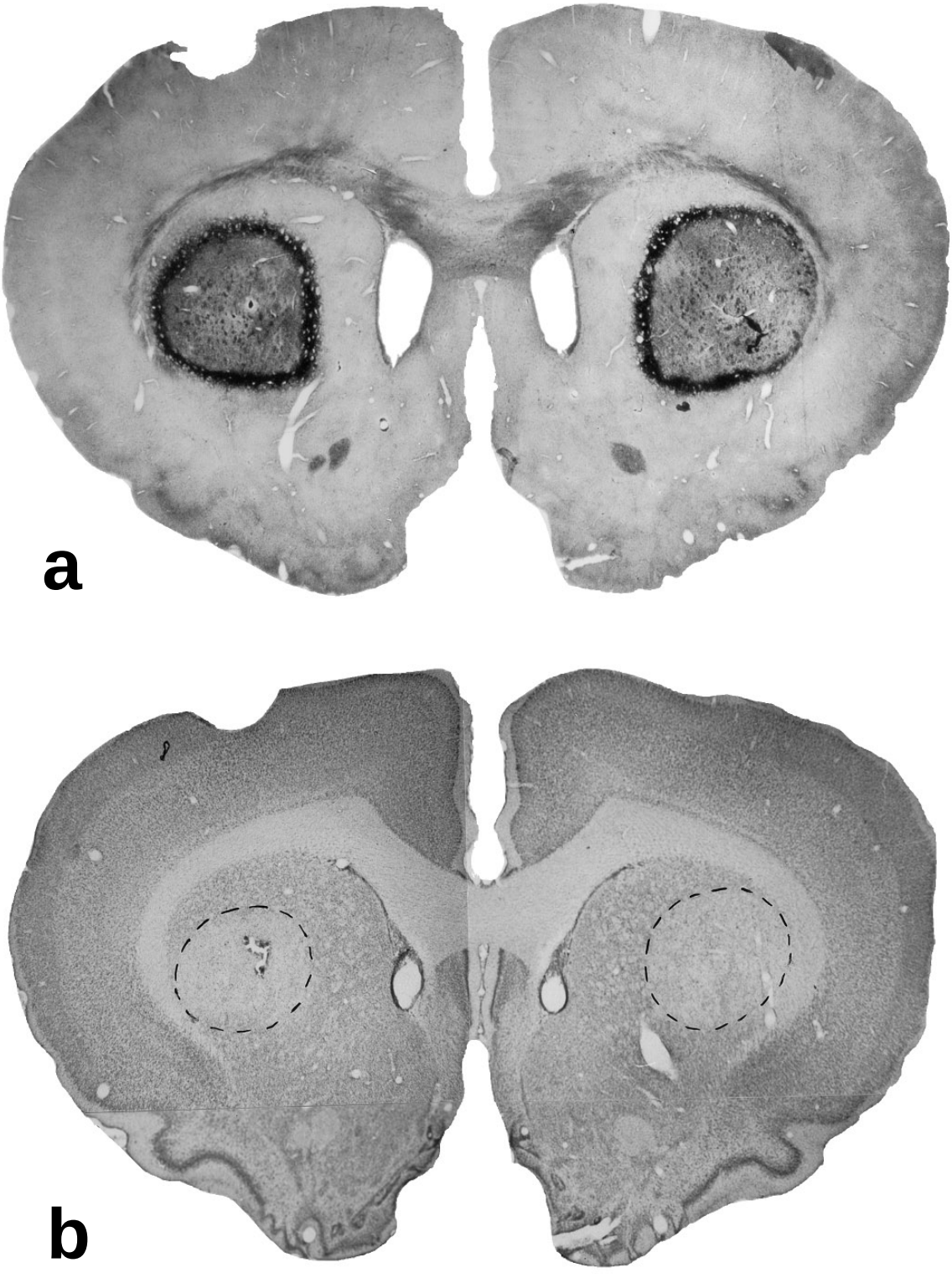

FIG. 6. Striatal neuronal damage following intraperitoneal administration of 3NPA. (a) Dark neuron-stained section showing dense, bilateral circles of silver-impregnated neurons and fibers in the caudate putamen. (b) Nissl-stained section showing bilateral circular areas of reduced staining (area inside dotted lines) in the caudate putamen.

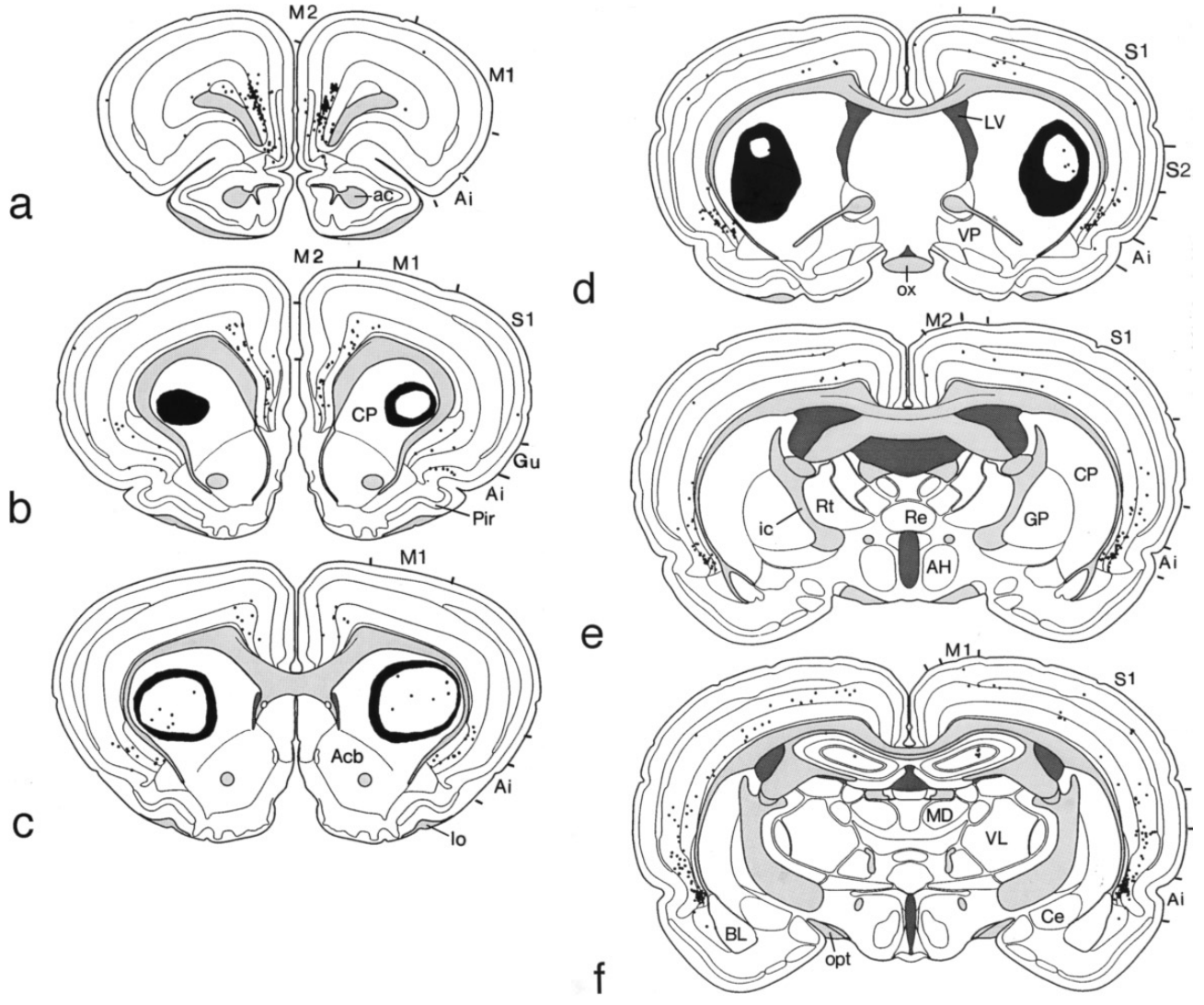

FIG. 7. Distribution of dark neurons following intraperitoneal injection of 3NPA as shown by plotting silver-impregnated neurons onto six coronal sections (a–f). Dots represent individual silver-impregnated neurons, while the area in full black in the caudate putamen (b–d) represents dense packing of dark neurons and fibers.

Pathological conditions such as head trauma, ischemia, insulin hypoglycemia, status epilepticus, and various neurotoxin-related damage seem to induce the same type of morphopathological changes that can be detected by a recently developed silver method of Gallyas (9, 28, 29, 38, 81). The similarity of the argyrophilic reaction of neurons of various origin after different types of injury suggests a common final cellular mechanism, the nature of which remains to be established. The reliable and predictable induction of somatic argyrophilia in specific neurons, the ability to visualize a large part of the dendritic tree that allows the classification of neuronal subtypes, the simultaneous staining of the projection axons of affected neurons, and the ability to follow the progression of pathological changes of affected neurons make this new Gallyas silver technique especially attractive in the evaluation of experimental models of neurodegenerative diseases.

Evaluation of Morphopathological Changes after Intracerebral 3NPA Injection

All 3NPA injection sites displayed a complete loss of tissue in the immediate vicinity of the injection and were surrounded by several dark cells. In addition, pronounced dark neuronal staining was observed in several thalamic nuclei, remote from the injection sites. There was negligible, if any, cell staining observed in control cases.

In the cases where 3NPA was injected into the FC, compromised neurons were found in the mediodorsal,

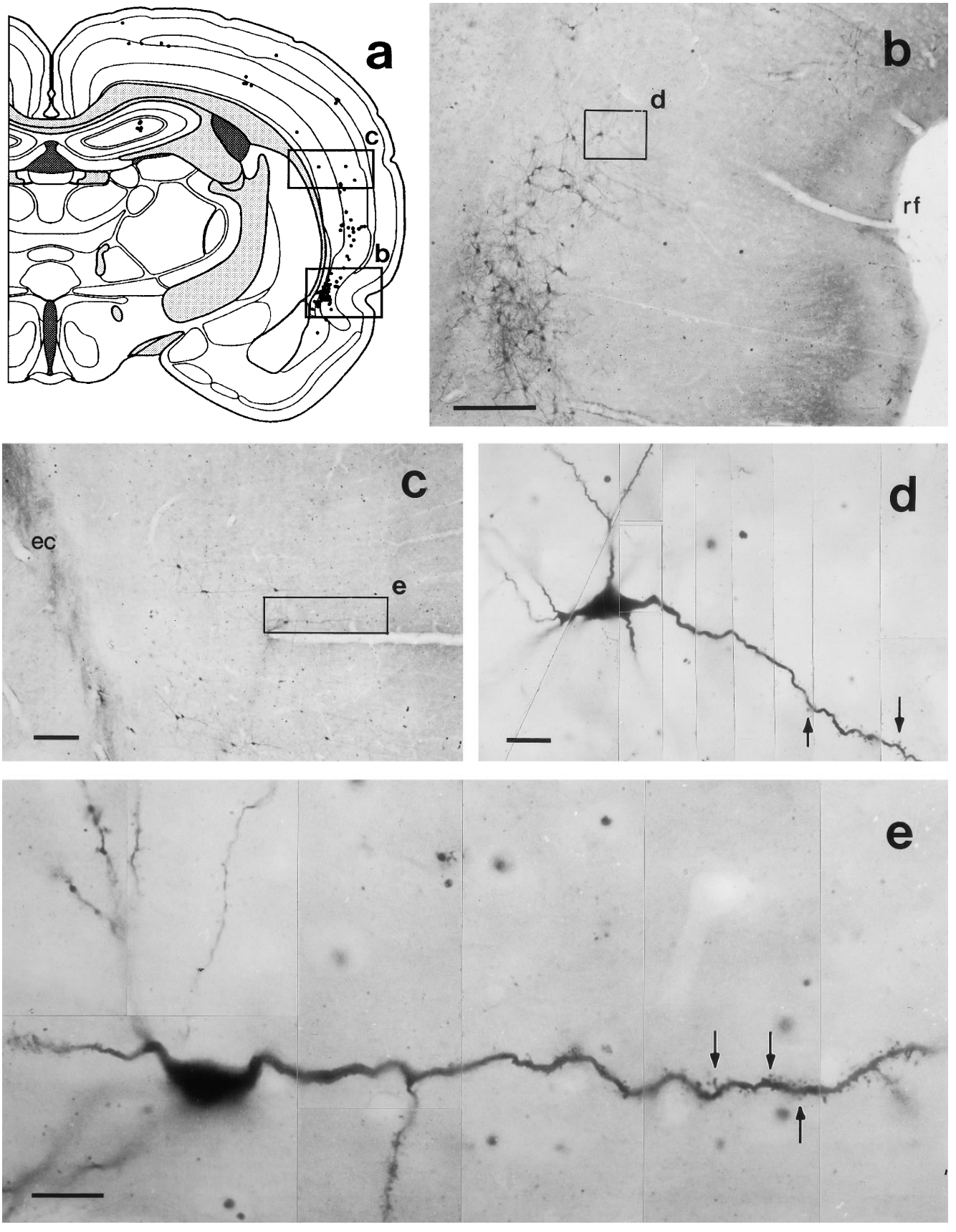

FIG. 8. Cortical neuronal damage following intraperitoneal injection of 3NPA. (a) Diagram showing distribution of labeled cells in the cortex at the level shown in Fig. 7f. Dots represent individual silver-impregnated cells. (b) Dark neurons in perirhinal cortex. (c) Dark neurons in the parietal cortex. (d) Dark pyramidal neuron from perirhinal cortex. (e) Dark pyramidal neuron from parietal cortex located in the boxed area in (c). Arrows, dendritic spines. Scale bar: b and c, 100 μm; d and e, 10 μm.

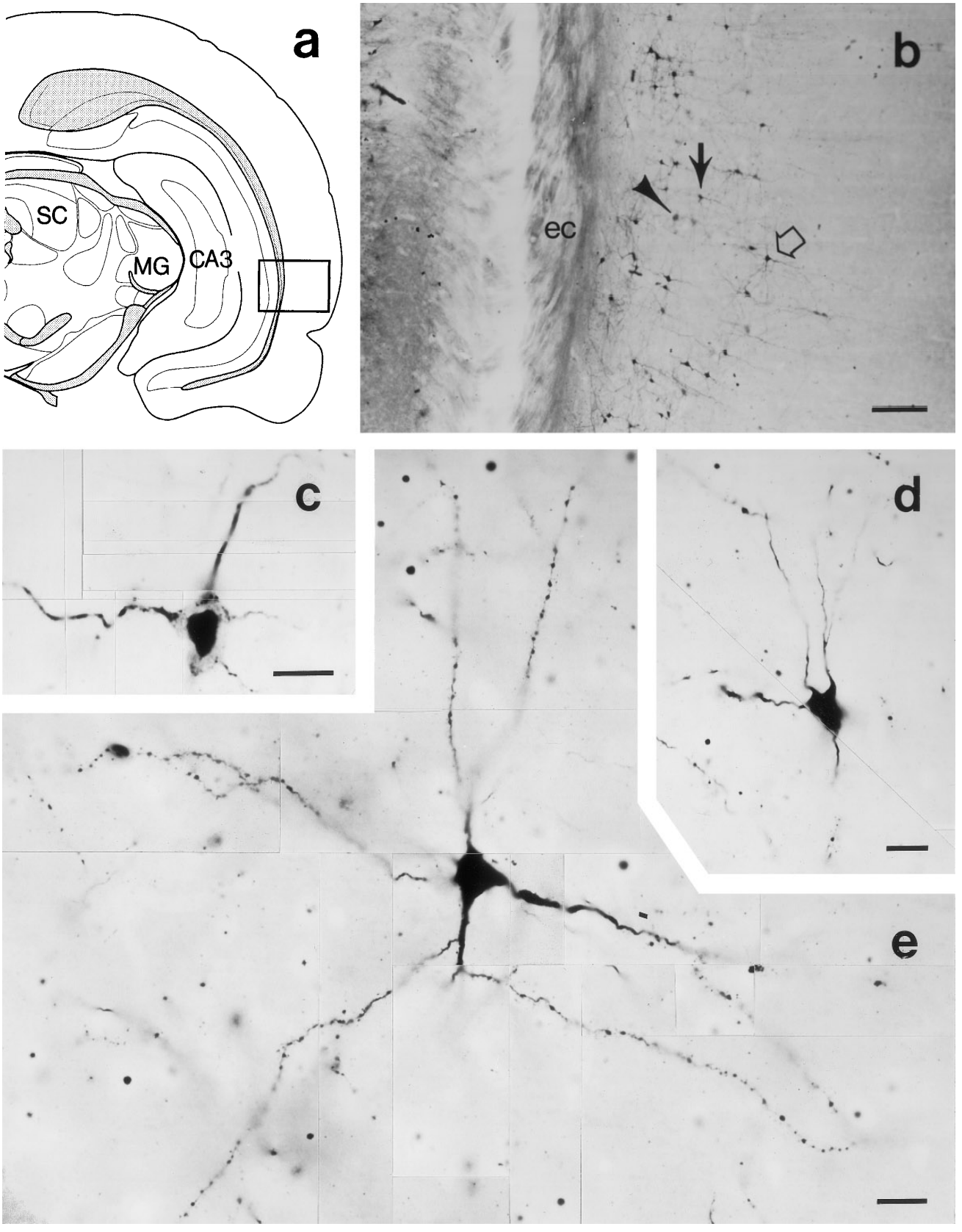

FIG. 9. Characteristics of silver-impregnated neurons in the temporal cortex following systemic administration of 3NPA. (a) Schematic approximately 5.6 mm posterior from the bregma. (b) Dark neurons taken from boxed area in (a). (c) Dark neuron at higher magnification, taken from (b) (filled arrow). Note the uneven dark neuronal staining of the perikaryon. (d) Dark neuron at higher magnification, taken from (b) (arrowhead). Note the full silver impregnation of perikaryon and processes. (e) Dark neuron at higher magnification, taken from (b) (open arrow). Note the beaded, disintegrating dendrites. Scale bar: b, 100 μm; c–e, 10 μm.

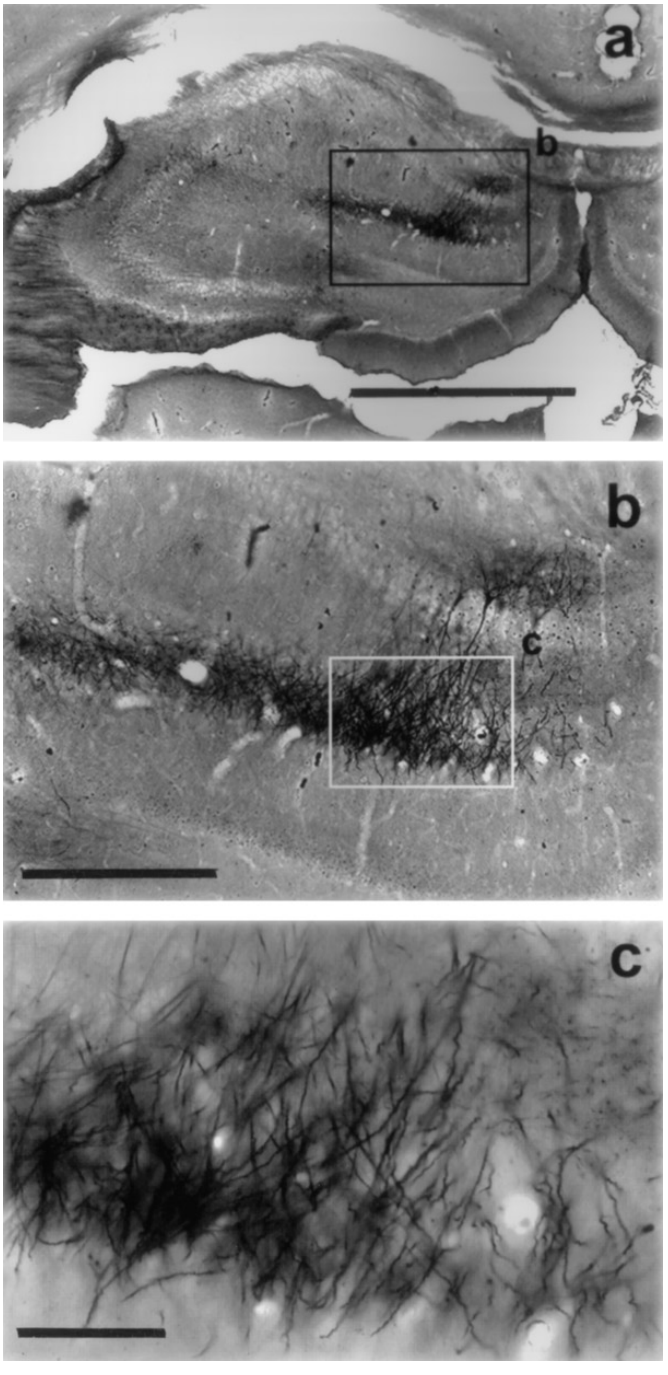

FIG. 10. Silver-impregnated cell bodies and dendritic processes in the hippocampus. (a) Low-magnification photomicrograph showing extensive involvement of the CA1 area. (b) Higher magnification of the boxed area of (a). Note the dense silver staining of the apical dendrites of pyramidal neurons in the stratum lacunosum–moleculare. (c) High-magnification view of apical dendrites of pyramidal cells from box in (b). Scale bar: a, 1 mm; b, 250 µm; c, 50 µm.

ventromedial, and ventrolateral thalamic nuclei, which are known to project to the anterior cingulate, to the medial precentral areas, and especially to the frontal motor cortex, areas that were all damaged by the two large injections into the frontal cortex (1, 15, 22, 34, 41, 46, 48, 70). However, we did not find evidence of compromised cells in the intralaminar nuclei, thalamic areas which project sparsely to the FC (10, 35, 46). Striatal 3NPA injection (Fig. 1b) resulted in dark neuronal staining in the intralaminar thalamic nuclei, which are known to project heavily to the striatum (10, 60, 67, 78, 83). Injection of 3NPA into the amygdala showed another distinct pattern of remote silver impregnation: dark neurons were observed among thalamic areas known to project to the amygdaloid body and posterior part of the CP (50, 63, 80). Also, the strong labeling in the paraventricular thalamic nucleus after ipsilateral BF injection is compatible with the heavy termination of paraventricular axons in the bed nucleus of stria terminalis, medial striatal areas adjacent to the lateral ventricle, and the nucleus accumbens (34, 58), regions which were heavily involved at the injection site. The above cases strongly suggest that thalamofugal neurons can be specifically affected by application of 3NPA into their terminal areas.

Whether this toxin can also affect neurons through damaged axons of passage is unclear; however, a number of observations suggest such a possibility. Fibers from the anterior thalamic nuclei pass through the medial part of CP and the cingulate bundle to terminate in different portions of the cingulate cortex (21, 75). The ipsilateral BF case resulted in a spillover of the 3NPA into the medial portion of the CP and the shaft passed through the cingulate bundle, which may account for the heavy neuronal staining in the anterior thalamic nuclei compared to the contralateral BF cases. Also, the labeling in the anterior nuclei in striatal injections may be due to 3NPA uptake into fibers of passage. In a similar fashion, fibers from the reuniens thalamic nucleus pass through the rostral part of the CP and medial compartment of the cingulate bundle as they travel toward the medial cortical surface (85). Dark neurons found in the laterodorsal thalamic nucleus in the striatal and ipsilateral BF cases may relate to damage of their axons as they pass through the CP and the deep white matter to enter into the cingulate cortex (82). In some cases, however, it is difficult to determine whether the observed labeling is due to the effect of the toxin at the terminal zone or through the preterminal portion of the axon. For example, it is well known that the mediodorsal thalamic nucleus sends projections to the prefrontal cortex and these fibers are passing through the medial portion of CP (34); however, there is not a general consensus in the literature (34, 69) whether mediodorsal fibers also terminate in the CP. On the other hand, the lack of labeling of the anterior, intralaminar, and rhomboid thalamic nuclei in FC cases, or the quantitative difference in the labeling of paraventricular thalamic cells between ipsilateral and contralateral BF cases, suggests that the labeling of the parent cell bodies may depend on a dense arborization of their terminals and/or injury of their axons in the

injection area. Perhaps a combined injection of 3NPA and a retrograde tracer, such as rhodamine-labeled latex beads that are known to be taken up less often by fibers of passage, needs to be done in order to determine the potential damage to fibers of passage by this toxin. Since there was no dark neuronal staining of cortical neurons after 3NPA injection into the internal capsule (Fig. 1e), heavily myelinated fibers may be less susceptible to this toxin.

Evaluation of Pathological Changes after Systemic 3NPA Administration

In addition to dark neuronal staining in the CP following ip injection, we also observed silver-impregnated cells in deep layers of various allo- and neocortical areas, including the hippocampal formation. The involvement of the deep cerebral cortex, especially in its lateral aspect subjacent to the rhinal sulcus, was previously noted after short survival of 3NPA treatments in rats, although the nature of this pathology was not described in detail perhaps due to the use of conventional hematoxylin and eosin (HE) staining (36). The medial prefrontal cortex, where many silver-impregnated neurons were detected, projects mainly to the medial part of the CP, including the nucleus accumbens and basal forebrain areas rich in corticopetal projection neurons (30, 43, 73, 88), territories which were free of diffuse neuronal insult. The insular cortex, another region which contained high number of argyrophilc neurons, projects primarily to the fundus striati, bed nucleus of the stria terminalis, amygdala, ventroposterior parvocellular thalamic nucleus, and brainstem visceromotor and viscerosensory nuclei (87). Finally, the perirhinal/ventral temporal cortex is considered a multimodal association area which projects to the amygdala (80). On the other hand, relatively few affected neurons were located in sensorimotor cortical areas, regions which project heavily to the lateral part of the CP (23, 55). In summary, the cortical neurons mostly affected in the systemic 3NPA cases with smaller striatal lesion do not seem to be part of the sensorimotor corticostriatal circuits but rather may be connected to limbic and autonomic centers and thus could represent an independent site of action of the toxin. On the other hand, in cases where a large proportion of the CP was included into the lesioned area, the impregnation of layer III pyramidal neurons may be the consequence of the primary striatal injury.

Potential Recovery and Selective Vulnerability of Neurons Following 3NPA Treatment

Unquestionably, the somatodendritic debris at the intracerebral injection sites as well as the shrunken, disintegrated neurons in the CP and some cortical areas after intraperitoneal 3NPA administration represents cell death as revealed by the loss of Nissl staining in adjacent sections. Whether or not the impregnated neurons at remote places from the intracerebral injections will eventually die or are simply transiently affected is a question of great importance, especially in evaluating the consequences of neuronal insult. Also, animals given the lower dose of 3NPA ip and longer survival period showed negligible dark neuronal staining and subsequent motor deficits, and, therefore, some of the staining may reflect a transient compromise of neurons, confirming a similar suggestion given by Allen *et al.* (4).

It is unclear why there are such localized lesions in the brain following ip 3NPA injection even though mitochondrial succinate dehydrogenase activity is reduced uniformly in all brain regions (31). Selective vulnerability of neurons may relate to neurochemical composition, lack of specific neurotrophic support, substantial glutamatergic input, altered excitatory amino acid receptor subtypes, and neural system-specific expression of genetic defects (2, 51, 56). Thalamic neurons are especially vulnerable after intracerebral administration of 3NPA, since corticofugal, striatonigral, and nigrostriatal neurons were not affected when 3NPA was injected into the internal capsule, the substantia nigra, or the CP, respectively, confirming other studies (4, 66). Moreover, we could not find dark neurons in the thalamus after similar large injections of kainic acid or *N*-methyl-D-aspartate (NMDA) into the frontal cortex (unpublished observations) which would suggest that 3NPA affects neurons both directly at the level of the cell body and at the axonal domain. This is compatible with the observation that thalamic neurons show retrograde degeneration due to damage of both their afferents and their parent axons (16).

The mechanism of striatal cell death after systemic administration of 3NPA is not well understood, although several factors may contribute to selective vulnerability of medium-sized spiny striatal neurons. Decortication, which removes putative glutamatergic inputs to the CP, can protect against 3NPA toxicity in the CP (6, 26), and NMDA receptors are upregulated in both cortex and CP following 3NPA injection (86). These are both lines of evidence for a secondary excitotoxic mechanism, in which endogeneous glutamate can become toxic following a compromise in the cell's energy levels (2, 62). However, NMDA antagonists such as MK-801 do not prevent 3NPA-induced neuronal damage (6), which suggests that 3NPA can produce neurodegeneration in both an NMDA receptor-dependent and -independent manner. The sparing of striatal nitric oxide synthase (NOS)-containing cells and the protection by NOS inhibitors against striatal lesions produced by systemic administration of 3NPA suggest a role of nitric oxide in 3NPA-induced neuronal degeneration (72). Since the tricarboxylic acid cycle of GABAer-

gic neurons is selectively inhibited by 3NPA (39), it is reasonable that the degeneration is primarily localized in the CP where the majority of neurons use GABA as their transmitter. Finally, a special vulnerability is given by the lateral striatal artery, by which, under conditions such as intoxication and energy deficiency, serum proteins from thrombosis and perivascular leakage may contribute to neuronal death that localizes specifically in the lateral CP (61). The hippocampal CA1 and CA3c pyramidal neurons that we have found affected by ip 3NPA seem to be the same neurons that are highly vulnerable to hypoxic insult (42). Future studies aimed at identifying the specific neurochemical composition and connectivity of degenerating neurons in 3NPA toxicity could reveal a more precise mechanism of the selective vulnerability of these neuronal populations.

3NPA and Modeling HD

Previously, other toxins have been used in modeling HD, including kainic acid, ibotenic acid, and quisqualic acid (8, 17, 25, 37, 54, 74). 3NPA has been introduced most recently in modeling HD, due to its destructive nature in both humans and animals which results in behavioral and neuropathological features comparable to those seen in HD (7, 52, 86). Additionally, energy metabolism may be compromised in HD patients (6), and since 3NPA is a mitochondrial toxin, perhaps a similar environment in which cellular energy levels are compromised can be duplicated. NOS/NADPH–diaphorase cells are selectively spared in HD (7) as well as after 3NPA treatment (11, 72). A final attractive characteristic of 3NPA that supports its use in modeling HD is its similar age-dependent nature: children are more susceptible to its toxic effects (52), similar to the clinical symptomatology which is more pronounced in patients with young-age onset than in those with the late-onset variant of the disease (59).

As a potential model of HD, our data are in agreement with several other studies suggesting that systemically administered 3NPA may be a better model of HD than intracerebral microinjection, given the simultaneous presence of striatal pathologies and motor deficits similar to what exists in HD (24). However, systemic administration induces marked variations in the neuropathological involvement of the CP in different species. The rodent systemic model showing neuropathology in the dorsolateral CP mimics well some of the motor deficits of HD. On the other hand, a recently developed chronic systemic 3NPA model in primates with a heavy involvement of the caudate nucleus (64) replicates more the cognitive deficits of HD. The expression of different symptoms in these animal models are in line with the differential roles of the multiple prefrontostriatal circuits in motor and cognitive functions (3). Since the early destruction of the periventricular portion of the caudate nuclei in HD effectively disconnects the prefrontal cortex from its target, its is likely that the cognitive and behavioral symptoms seen in HD are the result of the interruption of specific prefrontal–caudate circuits (18). As the disease progresses to affect more lateral areas of the CP (84), more motor symptoms develop due to the involvement of the corticoputaminal motor circuit. However, do cortical cells undergo retrograde degeneration due to removal of their targets in the CP? The cortical pathology in HD is somewhat controversial (47). While several studies have documented cortical atrophy and reduced glucose metabolism (49), especially in the prefrontal cortex in HD patients with depression (57), no specific cortical pathology was delineated and no damage was identified in the prefrontal cortex in the 3NPA primate model using conventional histological methods (64). More rigorous quantitative studies in HD, however, suggest a selective pattern of neuronal degeneration with substantial loss of layers III, V, and VI pyramidal neurons in the prefrontal cortex (40, 76, 77). Since neurons in layer VI project predominantly to the thalamus, claustrum, and other regions of the cerebral cortex, Hedreen *et al.* (40) concluded that it is unlikely that neurons in layer VI were lost as a result of retrograde degeneration secondary to striatal pathology. Our study also suggests that the relatively selective cortical pathology in rodents after systemic 3NPA treatment may not be the consequence of the diffuse pathology in the sensorimotor CP and therefore may represent another primary site of action of the toxin. On the other hand, the increased staining of layer III pyramidal neurons after the massive striatal lesion suggests the additional recruitment of corticostriatal neurons. In a careful neuropathological study, one brain in an advanced stage of HD displayed marked fibrillary astrocytosis in the temporal claustrum (84), in line with our observation in systemic 3NPA treatment, indicating that more targeted neuropathalogical studies are needed to disclose the full extent of cortical pathology in HD.

Thalamic atrophy and loss of neurons in some thalamic nuclei have been reported in earlier HD literature (20, 53). Thalamic metabolism in HD patients was normal in one PET study (49) but depressed in another (57). In a small proportion of rats with high doses of acute systemic 3NPA treatment, diffuse thalamic lesions were reported using HE staining (36) in agreement with occasional diffuse concentric argyrophilia in the laterodorsal thalamic nucleus in our systemic cases. In addition, the prominent degeneration of the various thalamofugal systems after intracerebral 3NPA injections in our studies and the presence of previously reported degenerating axons within the fiber tracts of the thalamus after systemic administration (4), both in cases with longer survival time, suggest thalamic involvement. It would be interesting to know whether the

thalamus is among the structures affected in HD and whether this is a consequence of the cortical or striatal pathology or represents an independent process. Similarly, given the differential vulnerability of the various hippocampal sectors to hypoxic damage (42) and the speculations of bioenergetic defects and excitotoxic-induced neurodegeneration in HD (2, 6), together with our current findings, there is the possibility of hippocampal insult in HD patients. It is hoped that further experimental studies with 3NPA using a combination of behavioral testing and a careful monitoring of the time course of degeneration in various neuronal systems may dissect the complex chain reaction leading to motor and cognitive symptoms seen in HD.

ACKNOWLEDGMENTS

The authors thank Mr. B. Lynch and Miss C. Waite for excellent technical assistance. This work was supported by Grants NS23945 and 30024.

REFERENCES

1. Aldes, L. D. 1988. Thalamic connectivity of rat somatic motor cortex. *Brain Res. Bull.* **20:** 333–348.
2. Albin, R. L., and T. Greenamyre. 1992. Alternate excitotoxic hypotheses. *Neurology* **42:** 733–738.
3. Alexander, G. E., M. D. Crutcher, and M. R. DeLong. 1990. Basal ganglia–thalamocortical circuits: Parallel substrates for motor, oculomotor, 'prefrontal' and 'limbic' functions. *Prog. Brain Res.* **1990:** 119–146.
4. Allen, C. N., J. L. Marino, and C. K. Meshul. 1994. 3-Nitropropionic acid (3-NPA)-induced axonal degeneration: A silver impregnation study. *Neurodegeneration* **3:** 225–234.
5. Andersson, P. B., V. H. Perry, and S. Gordon. 1991. The CNS acute inflammatory response to excitotoxic neuronal cell death. *Immunol. Lett.* **30:** 177–181.
6. Beal, M. F. 1992. Does impairment of energy metabolism result in excitotoxic neuronal death in neurodegenerative illnesses? *Ann. Neurol.* **31:** 119–130.
7. Beal, M. F., E. Brouillet, B. G. Jenkins, R. J. Ferrante, N. W. Kowall, J. M. Miller, E. Storey, R. Srivastava, B. R. Rosen, and B. T. Hyman. 1993. Neurochemical and histologic characterization of striatal excitotoxic lesions produced by the mitochondrial toxin 3-nitropropionic acid. *J. Neurosci.* **13:** 4186–4192.
8. Beal, M. F., R. J. Ferrante, K. J. Swartz, and N. W. Kowall. 1993. Chronic quinolinic acid lesions in rats closely resemble Huntington's disease. *J. Neurosci.* **11:** 1649–1659.
9. Beltramino, C. A., J. DeOlmos, F. Gallyas, L. Heimer, and L. Zaborszky. 1993. Silver impregnation as a tool for neurotoxic assessment. Pages 101–132 in L. Erinoff, Ed., *Assessing Neurotoxicity of Drugs of Abuse.* NIDA, Rockville, MD. [NIDA Monogr. Ser. 136]
10. Berendse, H. W., and H. J. Groenewegen. 1990. Organization of the thalamostriatal projections in the rat, with special emphasis on the ventral striatum. *J. Comp. Neurol.* **299:** 187–228.
11. Borlongan, C. V., T. K. Koutouzis, T. B. Freeman, D. W. Cahill, and P. R. Sanberg. 1995. Behavioral pathology induced by repeated systemic injections of 3-nitropropionic acid mimics the motoric symptoms of Huntington's disease. *Brain Res.* **697:** 254–257.
12. Borlongan, C. V., T. K. Koutouzis, T. S. Randall, T. B. Freeman, D. W. Cahill, and P. R. Sanberg. 1995. Systemic 3-nitropropionic acid: Behavioral deficits and striatal damage in adult rats. *Brain Res. Bull.* **36:** 549–556.
13. Brouillet, E., P. Hantraye, R. J. Ferrante, R. Dolan, A. Lerpy-Willig, N. W. Kowal, and E. F. Beal. 1995. Chronic mitochondrial energy impairment produces selective striatal degeneration and abnormal choreiform movements in primates. *Proc. Natl. Acad. Sci. USA* **92:** 7105–7109.
14. Coles, C. J., D. E. Edmondson, and T. P. Singer. 1979. Inactivation of succinate dehydrogenase by 3-nitropropionate. *J. Biol. Chem.* **254:** 5161–5167.
15. Cornwall, J., and O. T. Phillipson. 1988. Afferent projections to the dorsal thalamus of the rat as shown by retrograde lectin transport. I. The mediodorsal nucleus. *Neuroscience* **24:** 1035–1049.
16. Cowan, W. M. 1970. Anterograde and retrograde transneuronal degeneration in the central and peripheral nervous system. Pages 217–251 in W. J. H. Nauta and S. O. E. Ebbesson, Eds., *Contemporary Research Methods in Neuroanatomy.* Springer-Verlag, New York.
17. Coyle, J. T., and R. Schwarcz. 1976. Lesion of striatal neurones with kainic acid provides a model for Huntington's disease. *Nature* **263:** 244–246.
18. Cummings, J. L. 1993. Frontal–subcortical circuits and human behavior. *Arch. Neurol.* **50:** 873–880.
19. DiFiglia, M. 1990. Excitoxic injury of the neostriatum: A model for Huntington's disease. *Trends Neurosci.* **13:** 286–289.
20. Dom, R., M. Malfroid, and F. Baro. 1976. Neuropathology of Huntington's chorea: Studies of the ventrobasal complex of the thalamus. *Neurology* **26:** 64–68.
21. Domesick, V. B. 1972. Thalamic relationships of the medial cortex in the rat. *Brain Behav. Evol.* **6:** 457–483.
22. Donoghue, J. P., and C. Parham. 1983. Afferent connections of the lateral agranular field of the rat motor cortex. *J. Comp. Neurol.* **217:** 390–404.
23. Donoghue, J. P., and M. M. Herkenham. 1986. Neostriatal projections from individual cortical fields conform to histochemically distinct striatal compartments in the rat. *Brain Res.* **365:** 397–403.
24. Du, C., R. Hu, C. A. Csernansky, X. Z. Liu, C. Y. Hsu, and D. W. Choi. 1996. Additive neuroprotective effects of dextrorphan and cycloheximide in rats subjected to transient focal cerebral ischemia. *Brain Res.* **718:** 233–236.
25. Ferrante, R. J., N. W. Kowall, P. B. Cipolloni, E. Storey, and M. F. Beal. 1993. Excitotoxin lesions in primates as a model for Huntington's disease: Histopathologic and neurochemical characterization. *Exp. Neurol.* **119:** 46–71.
26. Fu, Y., F. He, S. Zhang, J. Huang, J. Zhang, and X. Jiao. 1995. 3-Nitropropionic acid produces indirect excitotoxic damage to rat striatum. *Neurotoxicol. Teratol.* **17:** 333–339.
27. Gallyas, F., J. R. Wolff, H. Bottcher, and L. Zaborszky. 1980. A reliable method for demonstrating axonal degeneration shortly after axotomy. *Stain Technol.* **55:** 291–297.
28. Gallyas, F., F. H. Guldner, G. Zoltay, and J. R. Wolff. 1990. Golgi-like demonstration of "dark" neurons with an argyrophil III method for experimental neuropathology. *Acta Neuropathol.* **79:** 620–628.
29. Gallyas, E., G. Zoltay, and Z. Horvath. 1992. Light microscopic response of neuronal somata, dendrites and axons to post-mortem concussive head injury. *Acta Neuropathol.* **83:** 499–503.
30. Gerfen, C. 1989. The neostriatal mosaic: Striatal patch-matrix organization is related to cortical lamination. *Science* **246:** 385–388.

31. Gould, D. H., and D. L. Gustine. 1982. Basal ganglia degeneration, myelin alternations, and enzyme inhibition induced in mice by the plant toxin 3-nitropropanoic acid. *Neuropathol. Appl. Neurobiol.* **8:** 377–393.
32. Graveland, G. A., R. S. Williams, and M. DiFiglia. 1985. Evidence for degenerative and regenerative changes in neostriatal spiny neurons in Huntington's disease. *Science* **227:** 770–773.
33. Greenamyre, J. T., and I. Shoulson. 1994. Huntington's disease. Pages 685–704 in D. Calne, Ed., *Neurodegenerative Diseases.* Saunders, Philadelphia.
34. Groenewegen, H. J. 1988. Organization of the afferent connections of the mediodorsal thalamic nucleus in the rat, related to the mediodorsal–prefrontal topography. *Neuroscience* **24:** 379–431.
35. Groenewegen, H. J., and H. W. Berendse. 1991. Restricted cortical termination fields of the midline and intralaminar thalamic nuclei in the rat. *Neuroscience* **42:** 73–102.
36. Hamilton, B. F., and D. H. Gould. 1987. Nature and distribution of brain lesions in rats intoxicated with 3-nitropropionic acid: A type of hypoxic (energy deficient) brain damage. *Acta Neuropathol.* **72:** 286–297.
37. Hantraye, P., D. Riche, M. Maziere, and O. Isacson. 1990. A primate model of Huntington's disease: Behavioral and anatomical studies of unilateral excitotoxic lesions of the caudate putamen in the baboon. *Exp. Neurol.* **108:** 91–104.
38. Harrison, M. B., G. F. Wooten, R. G. Willey, and L. Zaborszky. 1993. Degeneration of striatonigral neurons following volkensin injection in the substantia nigra. *Soc. Neurosci. Abstr.* **19:** 1587.
39. Hassel, B., and U. Sonnewald. 1995. Selective inhibition of the tricarboxylic acid cycle of GABAergic neurons with 3-nitropropionic acid in vivo. *J. Neurochem.* **65:** 1184–1191.
40. Hedreen, J. C., C. E. Peyser, S. E. Folstein, and C. A. Ross. 1991. Neuronal loss in layers V and VI of cerebral cortex in Huntington's disease. *Neurosci. Lett.* **133:** 257–261.
41. Herkenham, M. 1979. The afferent and efferent connections of the ventromedial thalamic nucleus in the rat. *J. Comp. Neurol.* **183:** 487–518.
42. Hsu, M., and G. Buzsaki. 1993. Vulnerability of mossy fiber targets in the rat hippocampus to forebrain ischemia. *J. Neurosci.* **13:** 3964–3970.
43. Hurley, K. M., H. Herbert, M. M. Moga, and C. B. Saper. 1991. Efferent projections of the infralimbic cortex of the rat. *J. Comp. Neurol.* **308:** 249–276.
44. Huntington's Disease Collaborative Research Group. 1993. A novel gene containing a trinucleotide repeat that is expanded and unstable on Huntington's disease chromosome. *Cell* **72:** 971–983.
45. Jeon, B. S., L. V. Jackson, and R. E. Burke. 1995. 6-Hydroxydopamine lesion of the rat substantia nigra: Time course and morphology of cell death. *Neurodegeneration* **4:** 131–137.
46. Jones, E. G., and R. Y. Leavitt. 1974. Retrograde axonal transport and the demonstration of non-specific projections to the cerebral cortex and striatum from thalamic intralaminar nuclei in the rat, cat and monkey. *J. Comp. Neurol.* **154:** 349–378.
47. Kowall, N. W., R. J. Ferrante, and J. B. Martin. 1987. Patterns of cell loss in Huntington's disease. *Trends Neurosci.* **10:** 24–29.
48. Krettek, J. E., and J. L. Price. 1978. The cortical projections of the mediodorsal nucleus and adjacent thalamic nuclei in the rat. *J. Comp. Neurol.* **171:** 157–192.
49. Kuwert, T., H. W. Lange, K. Langen, H. Herzog, A. Aulich, and L. E. Feinendegen. 1990. Cortical and subcortical glucose consumption measured by PET in patients with Huntington's disease. *Brain* **113:** 1405–1423.
50. LeDoux, J. E., and C. R. Farb. 1991. Neurons of the acoustic thalamus that project to the amygdala contain glutamate. *Neurosci. Lett.* **134:** 145–149.
51. Lees, G. J. 1993. Contributory mechanisms in the causation of neurodegenerative disorders. *Neuroscience* **54:** 287–322.
52. Ludolph, A. C., F. He, P. S. Spencer, J. Hammerstad, and M. Sabri. 1991. 3-Nitropropionic acid—Exogenous animal neurotoxin and possible human striatal toxin. *Can. J. Neurol. Sci.* **18:** 492–498.
53. McCaughey, W. T. E. 1961. The pathology spectrum of Huntington's chorea. *J. Nerv. Ment. Dis.* **133:** 91–103.
54. McGeer, E. G., and P. L. McGeer. 1976. Duplication of biochemical changes of Huntington's chorea by intrastriatal injections of glutamic and kainic acids. *Nature* **263:** 517–519.
55. McGeorge, A. J., and R. L. M. Faull. 1989. The organization of the projection from the cerebral cortex to the caudate putamen in the rat. *Neuroscience* **29:** 503–537.
56. Mattson, M. P. 1989. Cellular signaling mechanisms common to the development and degeneration of neuroarchitecture: A review. *Mech. Ageing Dev.* **50:** 103–157.
57. Mayberg, H. S., S. E. Starkstein, C. E. Peyser, J. Brandt, R. F. Dannals, and S. E. Folstein. 1992. Paralimbic frontal lobe hypometabolism in depression associated with Huntington's disease. *Neurology* **42:** 1791–1797.
58. Moga, M. M., R. P. Weiss, and R. Y. Moore. 1995. Efferent projections of the paraventricular thalamic nucleus in the rat. *J. Comp. Neurol.* **359:** 221–238.
59. Myers, R. H., J. P. Vonsattel, and T. J. Stevens. 1988. Clinical and neuropathological assessment of severity in Huntington's disease. *Neurology* **38:** 341–347.
60. Nguyen-Legros, J., P. Cesaro, B. Pollin, S. Laplante, and M. Gay. 1982. Thalamostriatal neurons with collateral projection onto the rostral reticular thalamic nucleus: Anatomical study in the rat by retrograde axonal transport of iron-dextran and horseradish peroxidase. *Brain Res.* **249:** 147–152.
61. Nishino, H., Y. Shimano, M. Kumazaki, and T. Sakurai. 1995. Chronically administered 3-nitropropionic acid induces striatal lesions attributed to dysfunction of the blood–brain barrier. *Neurosci. Lett.* **186:** 161–164.
62. Novelli, A., J. A. Reilly, P. G. Lysko, and R. C. Henneberry. 1988. Glutamate becomes neurotoxic via the *N*-methyl-D-aspartate receptor when intracellular energy levels are reduced. *Brain Res.* **451:** 205–212.
63. Ottersen, O. P., and Y. Ben-Ari. 1979. Afferent connections to the amygdaloid complex of the rat and cat. *J. Comp. Neurol.* **187:** 401–424.
64. Palfi, S., R. J. Ferrante, E. Brouillet, M. F. Beal, R. Dolan, M. C. Guyot, M. Peschanski, and P. Hantraye. 1996. Chronic 3-nitropropionic acid treatment in baboons replicates the cognitive and motor deficits of Huntington's disease. *J. Neurosci.* **16:** 3019–3025.
65. Paxinos, G., and C. Watson. 1986. *The Rat Brain in Stereotaxic Coordinates,* 2nd ed. Academic Press, San Diego.
66. Pei, G., and T. Ebendal. 1995. Specific lesions in the extrapyramidal system of the rat brain induced by 3-nitropropionic acid (3-NPA). *Exp. Neurol.* **132:** 105–115.
67. Phillipson, O. T., and A. C. Griffiths. 1985. The topographical order of inputs to nucleus accumbens in the rat. *Neuroscience* **16:** 275–296.
68. Pollard, H., M. C. Charriaut, S. Cantagrel, A. Represa, O. Robain, J. Moreau, and Y. Ben-Ari. 1994. Kainate-induced apoptotic cell death in hippocampal neurons. *Neuroscience* **63:** 7–18.

69. Price, J. 1995. Thalamus. Pages 629–648 in G. Paxinos, Ed., *The Rat Nervous System*, 2nd ed. Academic Press, San Diego.

70. Ray, J. P., and J. L. Price. 1992. The organization of the thalamocortical connections of the mediodorsal thalamic nucleus in the rat, related to the ventral forebrain–prefrontal cortex topography. *J. Comp. Neurol.* **323:** 167–197.

71. Reiner, A., R. L. Albin, K. D. Anderson, C. J. D'Amato, J. B. Penney, and A. B. Young. 1988. Differential loss of striatal projection neurons in Huntington's disease. *Proc. Natl. Acad. Sci. USA* **85:** 5733–5737.

72. Schulz, J. B., R. T. Mathews, B. G. Jenkins, R. J. Ferrante, D. Siwek, D. R. Henshaw, P. B. Cipolloni, P. Mecocci, N. W. Kowall, B. R. Rosen, and M. F. Beal. 1995. Blockade of neuronal nitric oxide synthase protects against excitotoxicity in vivo. *J. Neurosci.* **15:** 8419–8429.

73. Seasack, S. R., A. Y. Deutch, R. H. Roth, and B. S. Bunney. 1989. Topographical organization of the efferent projections of the medial prefrontal cortex in the rat: An anterograde tract-tracing study with *Phaseolus vulgaris* leucoagglutinin. *J. Comp. Neurol.* **290:** 213–242.

74. Schwarcz, R., W. O. Whetsell, and R. M. Mangano. 1983. Quinolinic acid: An endogenous metabolite that produces axon-sparing lesions in rat brain. *Science* **219:** 316–318.

75. Shibata, H. 1993. Efferent projections from the anterior thalamic nuclei to the cingulate cortex in the rat. *J. Comp. Neurol.* **330:** 533–542.

76. Storey, E., N. W. Kowall, S. F. Finn, M. F. Mazurek, and M. F. Beal. 1992. The cortical lesion of Huntington's disease: Further neurochemical characterization and reproduction of some of the histological and neurochemical features by *N*-methyl-D-aspartate lesions of rat cortex. *Ann. Neurol.* **32:** 526–534.

77. Storel, A., P. A. Paskevich, D. K. Kiely, E. D. Bird, R. S. Williams, and R. H. Myers. 1991. Morphometric analysis of the prefrontal cortex in Huntington's disease. *Neurology* **41:** 1117–1123.

78. Su, H., and M. Bentivoglio. 1990. Thalamic midline cell populations projecting to the nucleus accumbens, amygdala, and hippocampus in the rat. *J. Comp. Neurol.* **297:** 582–593.

79. Swanson, L. W. 1992. *Brain Maps: Structure of the Rat Brain*. Elsevier, New York.

80. Turner, B. H., and M. Herkenham. 1991. Thalamoamygdaloid projections in the rat: A test of the amygdala's role in sensory processing. *J. Comp. Neurol.* **313:** 295–325.

81. van den Pol, A. N., and F. Gallyas. 1990. Trauma-induced Golgi-like staining of neurons: A new approach to neuronal organization and response to injury. *J. Comp. Neurol.* **296:** 654–673.

82. Van Groen, T., and J. M. Wyss. 1992. Projections from the laterodorsal nucleus of the thalamus to the limbic and visual cortices in the rat. *J. Comp. Neurol.* **324:** 427–448.

83. Veening, J. G., F. M. Cornelissen, and P. A. J. M. Lieven. 1980. The topical organization of the afferents to the caudatoputamen of the rat: A horseradish peroxidase study. *Neuroscience* **5:** 1253–1268.

84. Vonsattel, J. P., R. H. Myers, T. J. Stevens, R. J. Ferrante, E. D. Bird, and E. P. Richardson. 1985. Neuropathological classification of Huntington's disease. *J. Neuropathol. Exp. Neurol.* **44:** 559–577.

85. Wouterlood, F. C., E. Saldana, and M. P. Witter. 1990. Projection from the nucleus reuniens thalami to the hippocampal region: Light and electron microscopic tracing study in the rat with the anterograde tracer Phaseolus vulgaris-leucoagglutinin. *J. Comp. Neurol.* **296:** 179–203.

86. Wullner, U., A. B. Young, J. B. Penney, and M. F. Beal. 1994. 3-Nitropropionic acid toxicity in the striatum. *J. Neurochem.* **63:** 1772–1781.

87. Yasui, Y., C. D. Breder, C. B. Saper, and D. F. Cechetto. 1991. Automatic responses and efferent pathways from the insular cortex in the rat. *J. Comp. Neurol.* **303:** 355–374.

88. Zaborszky, L., R. P. Gaykema, D. J. Swanson, and W. E. Cullinan. 1997. Cortical input to the basal forebrain. *Neuroscience.* [in press]